

Microwave-assisted switching of a nanomagnet: analytical determination of the optimal microwave field

N. Barros, H. Rassam, H. Kachkachi

Université de Perpignan Via Domitia,

52 Avenue Paul Alduy, 66860 Perpignan Cedex, France. and

PROMES - CNRS UPR8521, Tecnosud,

Rambla de la thermodynamique, 66100 Perpignan, France

Abstract

We analytically determine the optimal microwave field allowing to reverse the magnetic moment of a nanomagnet modeled as a macrospin. This is done by minimizing the total injected energy. The optimal field is found to be modulated both in amplitude and frequency, and orthogonal to the magnetic moment at any time. Its peculiar shape is directly related to the energy landscape (anisotropy, applied field) and to the damping parameter. For typical values of the damping parameter, a weak microwave field is sufficient to induce switching. The results are in good agreement with the fields previously obtained using the optimal control theory. The total injected energy is found to be proportional to the static energy barrier between the initial state and the saddle point and to the damping parameter. This result may be used as a means for probing the damping parameter and surface effects in real nanoparticles.

PACS numbers: 75.10.Hk, 75.75.Jn, 84.40.-x

I. INTRODUCTION

Magnetic recording is a key technology in the field of high density information storage. In order to increase thermal stability, small nanoparticles with high anisotropy may be used. However, high fields are then needed to reverse the magnetization but these are difficult to achieve in current devices. To overcome this so called magnetic recording trilemma, several solutions are being proposed. The most investigated route, and which already leads to industrial applications, is the heat-assisted magnetic recording¹. It consists in heating the particles by a laser which decreases the energy barrier between the two energy minima and thereby the switching fields. However, to avoid a loss of information, the heating must be very localized and followed by a very fast cooling, and as such these devices must be coupled to powerful heat dissipation systems.

An alternative solution is to assist the switching by a microwave (MW) field. In 2003 Thirion et al.² showed that the combination of a DC applied field (static field) well below the switching field with a small MW field pulse can reverse the magnetization of a nanoparticle. Further experimental and theoretical studies³⁻⁵ proved that this technique is more efficient if the frequency of the MW field matches the ferromagnetic resonance frequency of the nanoelements. The issue of state transition assisted by a MW field has previously been addressed in many areas of physics and chemistry, especially in the context of atomic physics. Furthermore, Meerson and Friedland⁶ studied the ionization of Rydberg atoms and predicted that a quasi-monochromatic oscillating electric field, whose frequency slowly decreases with time, should be far more efficient than a purely monochromatic field for achieving ionization. Measurements² and both analytical and numerical calculations^{7,8} have confirmed this fact for nanomagnets.

In our previous work⁹, we described a numerical method based on optimal control theory which renders an exact solution for the MW field that is necessary for the switching of a nanomagnet within a given potential energy. The formulation of this method consists in defining a cost functional and minimizing it using the conjugate gradient technique. Our results confirmed that a weak MW field, modulated both in amplitude and frequency, can induce the switching of the magnetization. Furthermore, the injected energy has been found to increase with damping.

The aim of the present study is to provide analytical expressions and to compare them with our numerical results, by using simple energy considerations. Moreover, the analytical developments presented here confirm the effects observed numerically and provide clear interpretations for the underlying physical processes. In the first part, we analytically determine the optimal MW field and show that it is directly related to the energy landscape (anisotropy, applied field) and to the

damping parameter. We then investigate the trajectory of the magnetization in the presence of the optimal field and show that it can be described by the Landau-Lifshitz-Gilbert equation with a negative damping parameter. In the second part, the analytical results are compared directly with the results obtained numerically using the optimal control theory.

II. ANALYTICAL CALCULATION OF THE OPTIMAL MICROWAVE FIELD

We consider a nanomagnet with homogeneous magnetization which can be modeled by a vector $\mathbf{M} = M_S \mathbf{m}$, where M_S is the saturation magnetization and $\|\mathbf{m}\| = 1$. This nanomagnet is characterized by a given anisotropy (uniaxial, biaxial, cubic...) and a damping parameter α . In the presence of a static magnetic field \mathbf{H} lower than the Stoner-Wohlfarth switching field, the potential energy surface presents several minima separated by saddle points.

At the initial time t_i , we assume that the magnetization is in a minimum $\mathbf{M}_i = M_S \mathbf{m}_i$. Adding a microwave (MW) field $\mathbf{B}(t)$ can then induce switching to another (final) minimum $\mathbf{M}_f = M_S \mathbf{m}_f$. Our aim is to find the optimal field $\mathbf{B}^{\text{opt}}(t)$ that achieves switching in a given time t_f while minimizing the energy injected into the system.

For the sake of simplicity, we introduce the reduced fields $\mathbf{h} \equiv \mathbf{H}/H_{\text{an}}$ and $\mathbf{b}(t) \equiv \mathbf{B}(t)/H_{\text{an}}$, where $H_{\text{an}} = 2K/\mu_0 M_s$ is the anisotropy field and K the anisotropy constant of the nanomagnet. We will also define the reduced time $\tau \equiv \gamma H_{\text{an}} t$, where $\gamma = 1.76 \times 10^{11} \text{ (T.s)}^{-1}$ is the gyromagnetic factor. For instance, for a cobalt particle of 3 nm diameter with $K \approx 2.2 \times 10^5 \text{ J.m}^{-3}$ and $M_s \approx 1.44 \times 10^6 \text{ A.m}^{-1}$ we have $\mu_0 H_{\text{an}} \approx 305 \text{ mT}$ and $t/\tau \approx 1.86 \times 10^{-11} \text{ s}$.

A. Energy and time trajectory in the presence of a microwave field

If only the static field is applied, the energy density of the system reads $\mathcal{E}_0(\mathbf{m}, \mathbf{h}) = \mathcal{E}_{\text{an}}(\mathbf{m}) - \mathbf{m} \cdot \mathbf{h}$ where \mathcal{E}_{an} is the anisotropy energy density. The reduced effective field is then defined by $\mathbf{h}_{\text{eff}} \equiv -\partial \mathcal{E}_0 / \partial \mathbf{m}$. If we add a MW field, the energy density becomes

$$\mathcal{E}(\mathbf{m}, \mathbf{h}, \mathbf{b}) = \mathcal{E}_{\text{an}}(\mathbf{m}) - \mathbf{m} \cdot (\mathbf{h} + \mathbf{b}(\tau)) \quad (1)$$

and the reduced total effective field now reads

$$\boldsymbol{\zeta}(\tau) \equiv -\frac{\partial \mathcal{E}}{\partial \mathbf{m}} = \mathbf{h}_{\text{eff}} + \mathbf{b}(\tau). \quad (2)$$

The time trajectory of the magnetization can be described by the driven Landau-Lifshitz-Gilbert equation

$$(1 + \alpha^2) \frac{d\mathbf{m}}{d\tau} = -\mathbf{m} \times \boldsymbol{\zeta}(\tau) - \alpha \mathbf{m} \times (\mathbf{m} \times \boldsymbol{\zeta}(\tau)). \quad (3)$$

This allows us to express the energy variation of the system as follows

$$\frac{d\mathcal{E}}{d\tau} = -\boldsymbol{\zeta}(\tau) \cdot \frac{d\mathbf{m}}{d\tau} - \mathbf{m} \cdot \frac{d\mathbf{b}}{d\tau} = -\mathbf{h}_{\text{eff}} \cdot \frac{d\mathbf{m}}{d\tau} - \frac{d}{d\tau} (\mathbf{m} \cdot \mathbf{b}). \quad (4)$$

Next, we define the mobile frame $(\mathbf{m}, \mathbf{u}, \mathbf{v})$ attached to the magnetization with $\mathbf{u} \equiv \mathbf{T}/T$ and $\mathbf{v} \equiv \mathbf{m} \times \mathbf{T}/T$, where $\mathbf{T} \equiv \mathbf{m} \times \mathbf{h}_{\text{eff}}$ and $T = \|\mathbf{m} \times \mathbf{h}_{\text{eff}}\|$. The MW field can then be decomposed as $\mathbf{b}(\tau) = b_m(\tau)\mathbf{m} + b_u(\tau)\mathbf{u} + b_v(\tau)\mathbf{v}$. In this frame, Eqs. (3) and (4) respectively become

$$(1 + \alpha^2) \frac{d\mathbf{m}}{d\tau} = \left(-1 + \frac{\alpha b_u + b_v}{T}\right) \mathbf{T} - \left(\alpha + \frac{b_u - \alpha b_v}{T}\right) (\mathbf{m} \times \mathbf{T}), \quad (5)$$

$$\frac{d\mathcal{E}}{d\tau} = \frac{-\alpha T - b_u + \alpha b_v}{1 + \alpha^2} T - \frac{db_m}{d\tau}. \quad (6)$$

We note that the parallel component of the MW field b_m has no direct effect on the magnetization trajectory and that its time derivative appears only in the energy variation.

B. Optimization of the MW field

In order to find the optimal MW field fulfilling the requirements described earlier we proceed in two steps. First, we define the critical MW field which allows us to maintain the precession of the magnetization by compensating the effects of damping (sec. II B 1). This field represents the lower limit for the optimal field sought. Using this result, we find the optimal MW field minimizing the injected energy (sec. II B 2) and check that it can induce switching of the magnetization (sec. II B 3).

1. MW field maintaining the precession

In order to induce switching the MW field must at least compensate for the effect of damping, which tends to take the magnetization back to the initial equilibrium position. If the compensation is complete the energy variation of the system $d\mathcal{E}/dt$ vanishes at any time thus reflecting the conservation of energy. According to Eq. (6) an infinity of MW fields leads to a full compensation

of damping. For instance, any field that is orthogonal to the magnetization so that $b_m = 0$ and satisfying the equation $-b_u + \alpha b_v = -\alpha T$ will do.

Among these MW fields the critical field can be defined as the one that minimizes the power injected in the system. The latter is proportional to the squared intensity of the MW field, i.e. $p_i(\tau) = \mathbf{b}^2(\tau) = b_m^2(\tau) + b_u^2(\tau) + b_v^2(\tau)$. Using the method of Lagrange multipliers we define the functional

$$L[b_m(\tau), b_u(\tau), b_v(\tau), \lambda(\tau)] = p_i^2(\tau) - \lambda(\tau) \frac{d\mathcal{E}}{d\tau}. \quad (7)$$

Assuming that $db_m(\tau)/d\tau$ does not depend explicetely on $b_m(\tau)$, the minimization of this functional leads to

$$\begin{aligned} b_m(\tau) &= 0, \\ b_u(\tau) &= -\frac{\alpha}{1 + \alpha^2} T, \\ b_v(\tau) &= \frac{\alpha^2}{1 + \alpha^2} T. \end{aligned} \quad (8)$$

The critical MW field thus reads

$$\mathbf{b}^{\text{crit}}(\tau) = \frac{\alpha}{1 + \alpha^2} [-\mathbf{T} + \alpha \mathbf{m} \times \mathbf{T}] \quad (9)$$

and the injected power is then

$$p_i^{\text{crit}}(\tau) = \frac{\alpha^2}{1 + \alpha^2} T^2. \quad (10)$$

In the presence of this MW field the magnetization precesses around the equilibrium position with a constant angle. This critical field represents a lower limit. Indeed, if the injected power is smaller than $p_i^{\text{crit}}(\tau)$ the magnetization goes back to the initial equilibrium position.

2. MW field minimizing the total injected energy

In order to minimize the total injected energy we have to make a few preliminary assumptions concerning the shape of the MW field. Considering the result of the previous section we limit our search to the family of MW fields defined by

$$\begin{aligned} b_m(\tau) &= \beta_m T \\ b_u(\tau) &= \beta_u T \\ b_v(\tau) &= \beta_v T \end{aligned}$$

where β_m , β_u and β_v are constant parameters. In the presence of such a MW field the energy variation reads

$$\frac{d\mathcal{E}}{d\tau} = \frac{-\alpha - \beta_u + \alpha\beta_v}{1 + \alpha^2} T^2 - \frac{db_m}{d\tau}. \quad (11)$$

The total energy injected to the system can be defined as $E = \int_{\tau_i}^{\tau_f} p_i(\tau) d\tau$. Therefore,

$$\begin{aligned} E &= \int_{\tau_i}^{\tau_f} (\beta_m^2 + \beta_u^2 + \beta_v^2) T^2 d\tau \\ &= \int_{\tau_i}^{\tau_f} (\beta_m^2 + \beta_u^2 + \beta_v^2) \left[\frac{1 + \alpha^2}{-\alpha - \beta_u + \alpha\beta_v} \left(\frac{d\mathcal{E}}{d\tau} + \frac{db_m}{d\tau} \right) \right] d\tau \\ &= \frac{(1 + \alpha^2) (\beta_m^2 + \beta_u^2 + \beta_v^2)}{-\alpha - \beta_u + \alpha\beta_v} [\mathcal{E}(\tau_f) - \mathcal{E}(\tau_i) + b_m(\tau_f) - b_m(\tau_i)]. \end{aligned} \quad (12)$$

Hence, the energy is minimal if $\beta_m = 0$, $\beta_u = -2\alpha/(1 + \alpha^2)$ and $\beta_v = 2\alpha^2/(1 + \alpha^2)$. Consequently, the optimal MW field is

$$\mathbf{b}^{\text{opt}}(\tau) = \frac{2\alpha}{1 + \alpha^2} [-\mathbf{T} + \alpha\mathbf{m} \times \mathbf{T}] = 2\mathbf{b}^{\text{crit}}(\tau). \quad (13)$$

The optimal field is twice the critical field determined previously, see Eq. (9). It is orthogonal to the magnetization at any time and its magnitude reads

$$\|\mathbf{b}^{\text{opt}}(\tau)\| = \frac{2\alpha}{\sqrt{1 + \alpha^2}} T. \quad (14)$$

The total injected energy is then

$$E = 4\alpha [\mathcal{E}(\tau_f) - \mathcal{E}(\tau_i)]. \quad (15)$$

According to these results, both the optimal field magnitude and the total injected energy increase with damping. This confirms the fact that the MW field must compensate for the effects of damping so as to induce switching.

3. Trajectory of the magnetization in presence of the optimal MW field

In order to check whether the optimal MW field obtained in the previous section induces switching of the magnetization as required, we now investigate the time trajectory of the magnetization. In the presence of this field, Eqs. (5) and (6) respectively become

$$(1 + \alpha^2) \frac{d\mathbf{m}}{d\tau} = -\mathbf{T} + \alpha\mathbf{m} \times \mathbf{T}, \quad (16)$$

$$\frac{d\mathcal{E}}{d\tau} = \frac{\alpha}{1 + \alpha^2} T^2. \quad (17)$$

The first equation is similar to the Landau-Lifshitz-Gilbert equation but with a negative damping parameter: it describes an *amplified* precession. The precession frequency is equal to the proper frequency of the magnetization. At any time the MW field is proportional to the derivative of the magnetization: $\mathbf{b}(t) = 2\alpha d\mathbf{m}/dt$. This is in agreement with the results of Sun et al.⁴.

At the minima and saddle points the effective field \mathbf{h}_{eff} is parallel to the magnetization so that $\mathbf{T} = \mathbf{0}$. Therefore, both the derivative of the magnetization and the MW field vanish. This has two consequences: (i) small fluctuations around the equilibrium position are necessary to start the amplified precession and (ii) the magnetization cannot cross a saddle point. The optimal MW field thus induces the motion of the magnetization from an initial state \mathbf{m}_i , close to an energy minimum, to a final state \mathbf{m}_f close to a saddle point. Fluctuations then allow the system to cross the saddle point and afterwards the damping takes up to lead the magnetization down to the second energy minimum. If the energy landscape is complex with several barriers successive pulses may then be necessary to induce switching.

At both the initial and the final states the MW field is close to zero. The difference $\mathcal{E}(\tau_f) - \mathcal{E}(\tau_i)$ is thus close to the static energy barrier between the saddle point and the initial state $\Delta\mathcal{E}_0 = \mathcal{E}_0(\tau_f) - \mathcal{E}_0(\tau_i)$ and Eq. (15) becomes

$$E = 4\alpha \Delta\mathcal{E}_0. \quad (18)$$

The total injected energy is therefore proportional to the energy barrier to be overcome. Hence, if the static field is close to the switching field, a very weak MW field can induce switching.

C. Uniaxial anisotropy and longitudinal static field

In this section we study the trajectory of the magnetization in the presence of the optimal MW field for a nanoparticle with uniaxial anisotropy and a longitudinal static field.

We consider a nanomagnet with uniaxial anisotropy with easy axis in the z direction. The anisotropy energy density is then $\mathcal{E}_{\text{an}}(m_z) = -k m_z^2/2$ with $k = 1$. The static field is applied in the $(-z)$ direction with a magnitude $0 \leq h < k$. The magnetization is initially close to the metastable minimum and its z component is thus $m_0 \equiv m_z(\tau_i = 0) \approx 1$. Setting $x = h/k$, the static energy of the system is

$$\mathcal{E}_0(m_z) = k \left(-\frac{m_z^2}{2} + x m_z \right). \quad (19)$$

The saddle point then corresponds to $m_z = x$, so the static energy barrier between the latter and the initial metastable state is $\Delta\mathcal{E}_0 = k(1-x)^2/2$.

For this system, the effective field reads $\mathbf{h}_{\text{eff}} = k(-x + m_z)\mathbf{e}_z$. Projecting Eq. (16) onto the z axis then yields

$$\frac{dm_z}{d\tau} = \frac{\alpha}{1+\alpha^2} (\mathbf{m} \times \mathbf{T}) \cdot \mathbf{e}_z = -\frac{\alpha k}{1+\alpha^2} (-x + m_z) (1 - m_z^2). \quad (20)$$

In order to simplify the expressions we introduce the integral

$$I(m_z) = \int_0^{m_z} \frac{-du}{(-x+u)(1-u^2)} = \frac{1}{2(1-x^2)} \ln \left[\frac{(1+m_z)^{1-x} (1-m_z)^{1+x}}{(-x+m_z)^2} \right] + C^{te}. \quad (21)$$

Solving Eq. (20) with the initial condition $m_z(t=0) = m_0$ leads to the equation

$$I(m_z) - I(m_0) = \frac{\alpha k}{1+\alpha^2} \tau. \quad (22)$$

This equation can be analytically solved for m_z only if $x = 0$ (no static field). Otherwise, the evolution of m_z with time can be obtained numerically, see Fig. 1. As predicted previously, for long times the magnetization goes towards to the saddle point but never reaches it since $I(m_z)$ diverges for $m_z = x$.

>From Eq. (14) we can express the optimal MW field intensity in terms of m_z as follows

$$\|\mathbf{b}^{\text{opt}}(m_z)\| = \frac{2\alpha k}{\sqrt{1+\alpha^2}} (-x + m_z) \sqrt{1 - m_z^2}. \quad (23)$$

The time evolution of the MW field intensity is plotted in Fig. 1. We note that the pulses follow neither a Gaussian nor a Lorentzian function. The peak intensity is reached for $m_z = \frac{1}{4}(x + \sqrt{8+x^2})$ and is given by

$$b_{\text{max}}^{\text{opt}} = \frac{\alpha k}{2\sqrt{1+\alpha^2}} \left(-3x + \sqrt{8+x^2} \right) \sqrt{1 - \frac{(x + \sqrt{8+x^2})^2}{16}}. \quad (24)$$

>From this, we can see that the peak intensity $b_{\text{max}}^{\text{opt}}$ decreases with x (see Fig. 6). Indeed, for higher magnitudes of the static field, the energy barrier $\Delta\mathcal{E}_0$ between the metastable state and the saddle point is lower, so that a lower energy is needed to reach the saddle point. Since $0 \leq x < 1$ the peak intensity is limited as follows

$$b_{\text{max}}^{\text{opt}} < \frac{\sqrt{2}\alpha k}{\sqrt{1+\alpha^2}}. \quad (25)$$

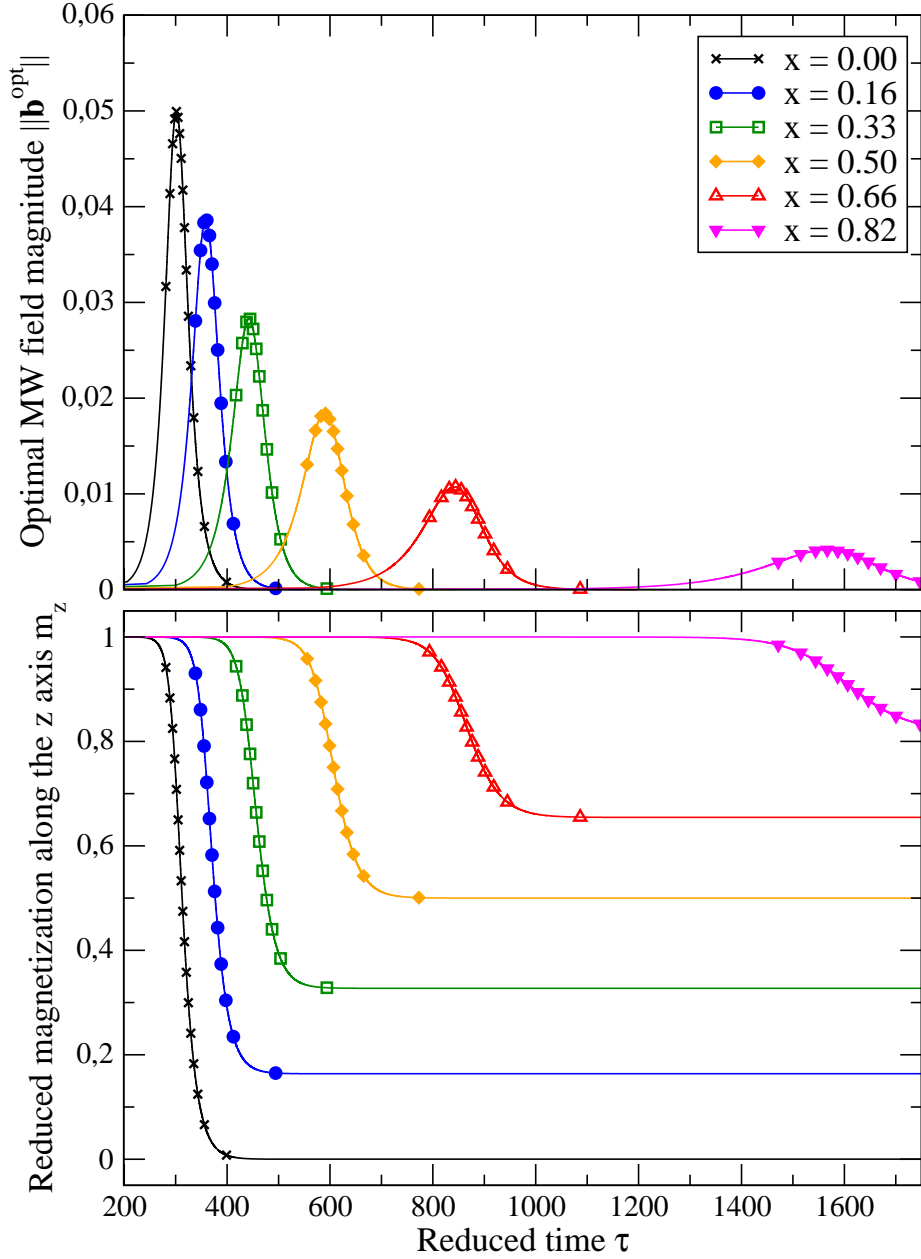


Figure 1: Optimal MW field intensity $\|\mathbf{b}^{\text{opt}}(\tau)\|$ (upper panel) and trajectory of the magnetization $m_z(\tau)$ (lower panel) for a longitudinal static field with magnitude $x = h/k$. Parameters: $\alpha = 0.05$, $m_0 = 0.99998$.

Hence, for low values of the damping parameter α , the intensity of the optimal MW field is small. This fully confirms the results of our numerical study⁹. Using Eqs. (21) and (23), we can also obtain analytically the peak duration $\Delta\tau$, defined as the full width at half maximum

$$\Delta\tau = \frac{1 + \alpha^2}{\alpha k} g(x), \quad (26)$$

where $g(x)$ is a cumbersome function of x . This characteristic time increases with x (see Fig. 6). For high values of x , the switching will thus require a very low field but a very long time, as can be seen in Fig. 1. Moreover, the characteristic time decreases with damping.

The area below the curves $\|\mathbf{b}^{\text{opt}}(\tau)\|$ is

$$\begin{aligned} A &= \int_{t=0}^{t=\infty} \|\mathbf{b}^{\text{opt}}(\tau)\| d\tau = \int_{m_z=m_0}^{m_z=x} \|\mathbf{b}^{\text{opt}}(m_z)\| \frac{d\tau}{dm_z} dm_z \\ &= 2\sqrt{1+\alpha^2} [\arccos(x) - \arccos(m_0)] = 2\sqrt{1+\alpha^2} (\theta_f - \theta_i). \end{aligned} \quad (27)$$

where θ_i and θ_f are the polar angles of the magnetization respectively at the initial state and saddle point. This area is thus proportional to the “angular distance” that the magnetization must cross to reach the saddle point. For increasing values of the static field magnitude x , this area decreases since the saddle point comes closer to the initial state.

The z component of \mathbf{b}^{opt} , given by Eq. (13), is

$$b_z^{\text{opt}}(m_z) = -\frac{2\alpha^2 k}{1+\alpha^2} (-x + m_z) (1 - m_z^2). \quad (28)$$

>From Eq. (23) we can see that the ratio $|b_z^{\text{opt}}(m_z)| / \|\mathbf{b}^{\text{opt}}(m_z)\|$ is $\frac{\alpha}{\sqrt{1+\alpha^2}} \sqrt{(1 - m_z^2)}$, whose upper limit is $\frac{\alpha}{\sqrt{1+\alpha^2}}$. Consequently, for small values of the damping parameter α , the component of the time-dependent field along the anisotropy easy axis can be neglected and the optimal field lies in the xy plane.

We now define the precession phase of the magnetization as $\varphi(\tau) = \arctan(m_y(\tau)/m_x(\tau))$. Projecting Eq. (16) on the x and y axes leads to the relation

$$\omega(t) = \frac{d\varphi}{d\tau} = \frac{\|\mathbf{h}_{\text{eff}}\|}{1+\alpha^2} = \frac{k}{1+\alpha^2} (-x + m_z). \quad (29)$$

This precession frequency is equal to the proper frequency of the magnetization, obtained by solving Eq. 3 in the absence of a MW field. At the initial state, the precession frequency is close to the FMR frequency $\omega_{\text{FMR}} = k(1 - x)/(1 + \alpha^2)$. It then decreases towards zero, following the curvature of the energy well.

For small values of α , the optimal field lies in the xy plane and its phase can be defined by $\tilde{\varphi}(t) = \arctan(b_y^{\text{opt}}(t)/b_x^{\text{opt}}(t))$. It can be shown that

$$\tan \tilde{\varphi}(\tau) = \frac{m_x(\tau) + \alpha m_y(\tau) m_z(\tau)}{-m_y(\tau) + \alpha m_x(\tau) m_z(\tau)} \approx -\frac{m_x(\tau)}{m_y(\tau)} = \cot \varphi(\tau). \quad (30)$$

This implies that the time-dependent field and the magnetization are synchronized with $\tilde{\varphi}(\tau) \approx \varphi(\tau) + \pi/2$. Hence, the frequency of the time-dependent field is equal to the proper precession frequency of the magnetization.

Finally, using Eqs. (20) and (23), the total injected energy can be computed. As shown previously in Eq. (18), it is proportional to the damping parameter and to the energy barrier $\Delta\mathcal{E}_0$.

$$E = \int_0^{+\infty} \left\| \mathbf{b}^{\text{opt}}(\tau) \right\|^2 d\tau = 2\alpha k (x - 1)^2 = 4\alpha\Delta\mathcal{E}_0. \quad (31)$$

III. COMPARISON WITH THE NUMERICAL RESULTS

In order to check the validity of our model, we have carried out numerical calculations based on the optimal control theory, as presented in⁹. Our model system is a particle with uniaxial anisotropy along the z axis with $k = 1$. The numerical method consists in minimizing the cost functional

$$\mathcal{F}[\mathbf{m}(\tau), \mathbf{b}(\tau)] = \frac{1}{2} \|\mathbf{m}(\tau_f) - \mathbf{m}_f\|^2 + \frac{\eta}{2} \int_0^{\tau_f} d\tau \mathbf{b}^2(\tau)$$

along the trajectory given by the Landau-Lifshitz-Gilbert equation (3), with \mathbf{m}_f is the target magnetization (stable minimum), $\mathbf{m}(\tau_f)$ is the magnetization reached at time τ_f and η is a numerical control parameter. The numerical problem is solved using the modified conjugate gradient technique supplemented by a Metropolis algorithm.

Unless otherwise specified, the numerical parameters used in the current study are: initial reduced time $\tau_i = 0$, final reduced time $\tau_f = 800$ (corresponding to a few ns in real time), number of points $N = 15000$, so the sampling time $(\tau_f - \tau_i)/(N - 1)$ is about 0.05; damping parameter $\alpha = 0.05$; control parameter $\eta = 0.01$. For a better comparison with the analytical results, the MW field was allowed to move in any direction during the optimization.

A. Reference calculation

A first numerical optimization was carried out for a static field with magnitude $h = 0.5$ ($x = 0.5$) applied in the $(-z)$ direction. The results are in good agreement with the analytical calculations of part II. As can be seen in Fig. 2, the optimal MW field is modulated both in amplitude and frequency. The MW field is mainly in the xy plane and its magnitude is small (less than 0.03, corresponding to a few mT in real field) as expected since the damping parameter is small. The pulse starts at about $\tau = 350$ and vanishes as soon as the magnetization crosses the saddle point (at about $\tau = 670$). Next, the damping takes up to lead the magnetization to the more stable energy minimum.

Fig. 3 shows that the MW field intensity obtained numerically is in good agreement with the analytical result in Eq. (23). From $\tau \approx 570$, the MW field intensity is slightly higher numerically, which induces m_z to decrease faster and finally the magnetization to cross the saddle point. Fig. 4 confirms that the magnetization precession and the MW field are synchronized, the initial frequency being close to the FMR frequency. The time evolution of the frequency is similar to the evolution of m_z (Fig.3), since both values are related by Eq. (29). Consequently, after $\tau \approx 570$ the numerical frequency is lower than the analytical frequency.

B. Effect of the static field magnitude and direction

The MW field $\mathbf{b}(\tau)$ has been optimized numerically for several magnitudes and orientations of the static field \mathbf{h} . For each configuration, the energy barrier $\Delta\mathcal{E}_0$ and the total injected energy $E = \int_{\tau_i}^{\tau_f} \|\mathbf{b}^{\text{opt}}(\tau)\|^2 d\tau$ have been computed numerically, and are reported in Fig. 5. As predicted analytically by Eq. (18), the injected energy is found to be proportional to the energy barrier and to 4α .

In the case of a static field applied along $(-z)$, the shape of the pulse can be directly compared with the analytical results of sec. II C, see Fig. 6. The numerical and analytical results are in good agreement. As expected, the maximal peak intensity $b_{\text{max}}^{\text{opt}}$ decreases and the pulse duration $\Delta\tau$ increases rapidly when the magnitude of the static field x increases.

C. Effect of damping

As predicted by Eqs. (18) and (31), for a given static energy barrier $\Delta\mathcal{E}_0$, the injected energy is proportional to the damping parameter α . This has been checked numerically by varying the damping parameter from 0.015 to 0.30 (Fig. 7). In these calculations, the static field \mathbf{h} is applied in the $(-z)$ direction with the magnitude $x = 0.5$.

Fig. 8 shows that for low values of α , the pulses height decreases but their duration increases, in agreement with Eqs. (24) and (26). For an undamped system, the switching should thus be infinitely long, so our analytical and numerical methods are not adapted to describe such a system.

As can be observed, for very low values of the damping parameter α , a discrepancy between the analytical calculations and the numerical optimization is observed. Indeed, since the optimal peak duration becomes very long, the number of numerical points N must be increased, so the conjugate gradient algorithm becomes less efficient. However, as can be seen in Fig. 7, this discrepancy has

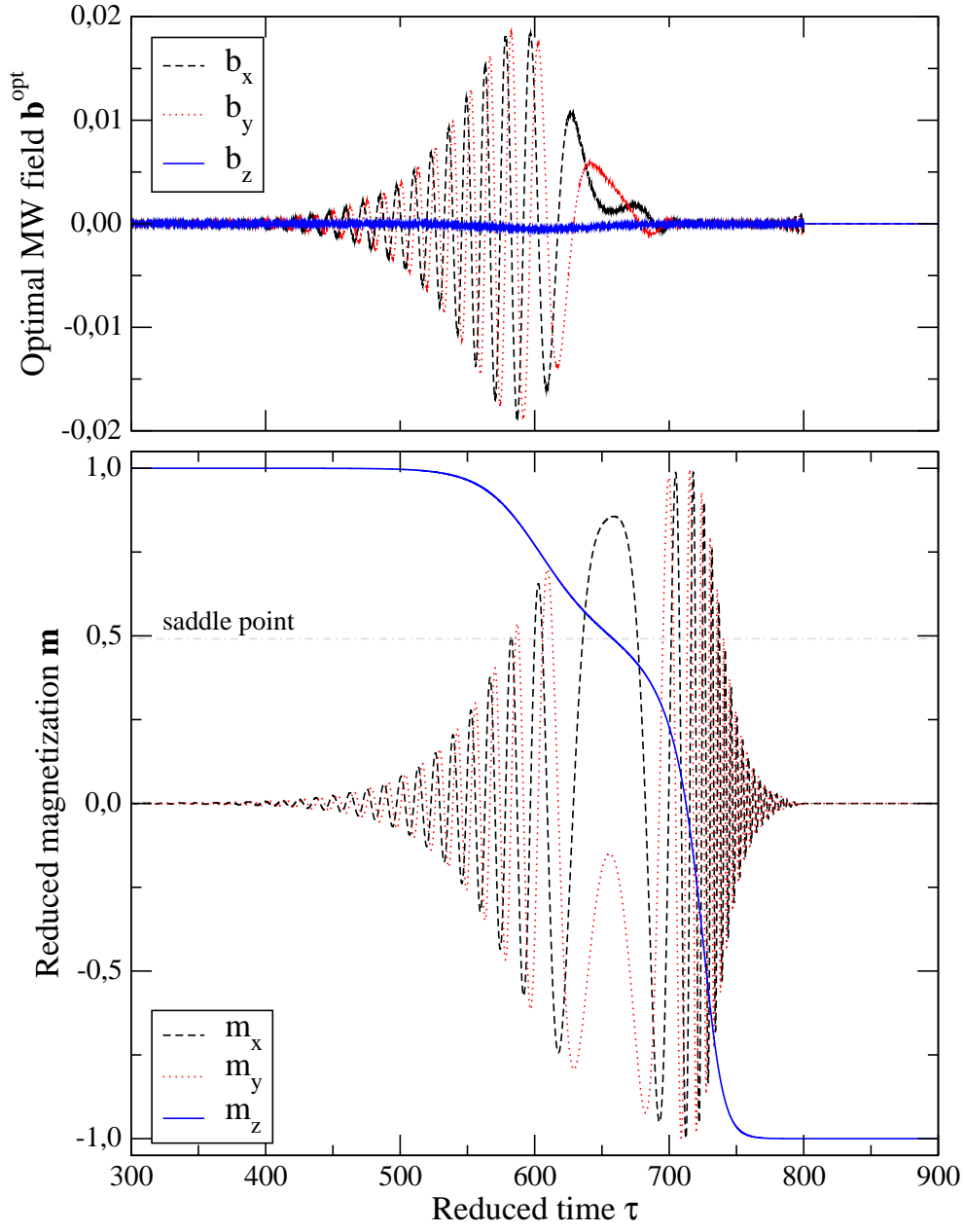


Figure 2: Numerical results for the reference calculation: optimal MW field (upper panel) and magnetization time trajectory (lower panel).

a negligible effect on the injected energy.

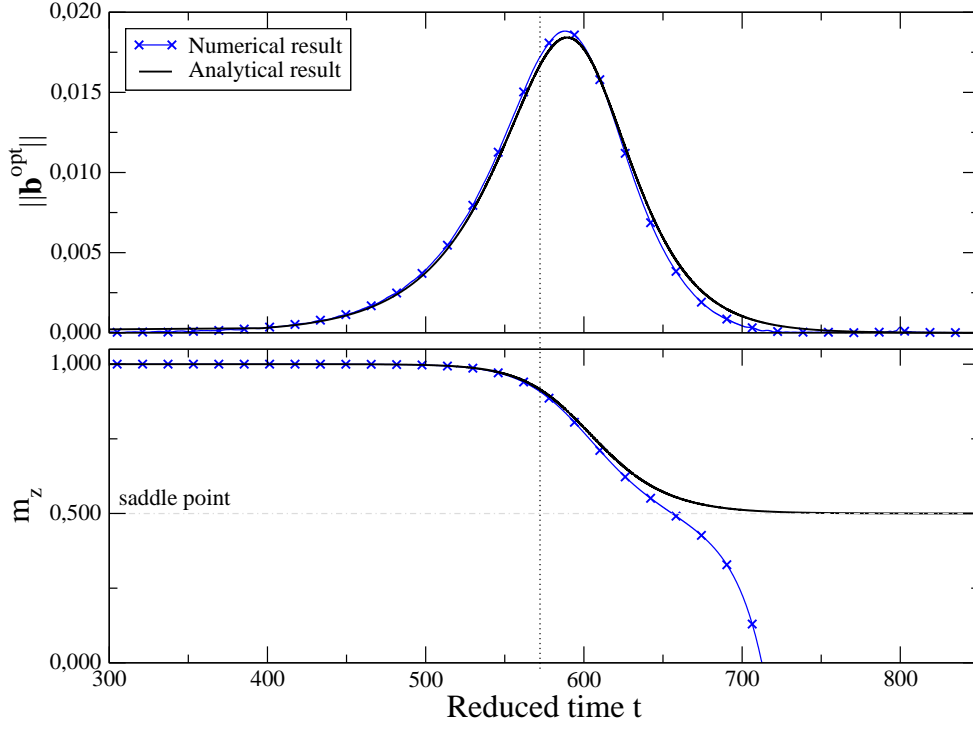


Figure 3: Comparison between the analytical and numerical results for the reference calculation: optimal MW field magnitude $\|\mathbf{b}^{\text{opt}}\|$ (higher panel) and z component of the magnetization (lower panel).

IV. CONCLUSION

We determined analytically the optimal microwave field allowing for the switching of the magnetization of a monodomain nanoparticle with uniaxial anisotropy while minimizing the injected energy. This study provides a clear interpretation of the results obtained numerically using the optimal control theory⁹, especially the simple dependence of the pulse on the damping parameter.

Our results show that the optimal MW field is modulated both in amplitude and frequency, and is directly proportional to the derivative of the magnetization. For typical values of the damping parameter ($\alpha < 1$), a weak MW field is sufficient to induce switching. Its role is to drive the magnetization from the initial state towards the saddle point; the time trajectory of the magnetization can then be described as an amplified precession. After crossing the saddle point the damping induces the relaxation to the final state. The injected energy is then proportional to the damping parameter and to the static energy barrier between the initial state and the saddle point.

For a nanomagnet with uniaxial anisotropy placed in a longitudinal static field, the shape of

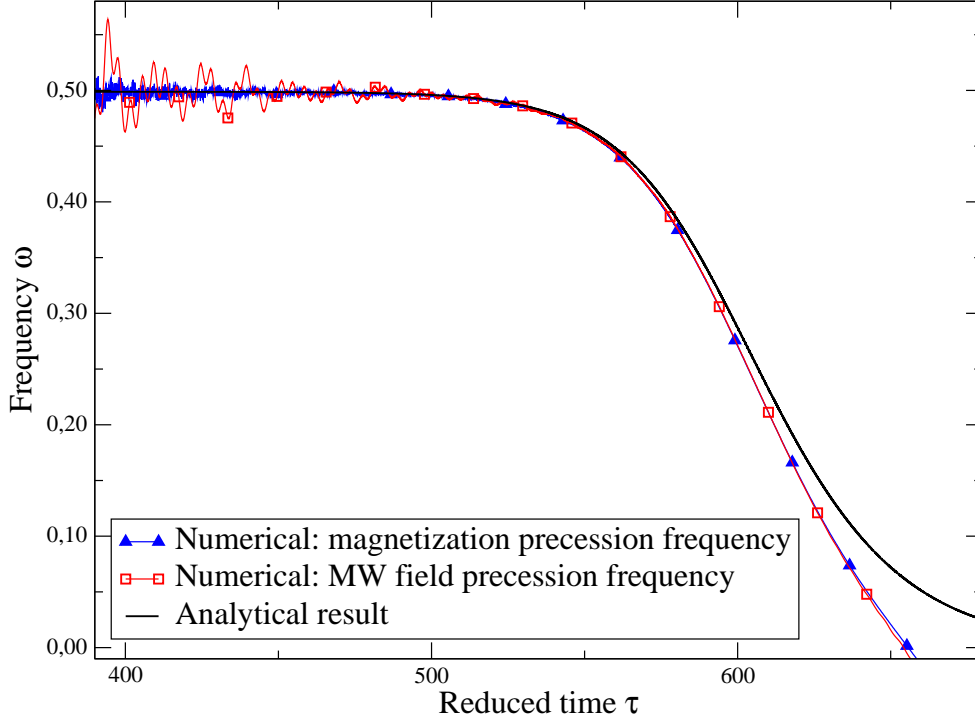


Figure 4: Comparison between the analytical and numerical results for the reference calculation: precession frequencies of the magnetization and MW field.

the MW field pulse has been obtained analytically. We have shown that the optimal MW field pulse becomes smaller but much more spread when the damping decreases.

In the case of more complex energy landscapes (biaxial or cubic anisotropies), the switching is likely to be triggered by a succession of MW field pulses. This hypothesis will be later tested numerically. This study could then be extended to small nanomagnets where surface effects can not be neglected, using the effective one-spin model (EOSP)^{10–12}.

The MW fields that we optimized have an amplitude and a frequency which vary slowly, and can be reproduced experimentally using a frequency generator. Consequently, our theoretical results could be used to probe the damping parameter and assess the role of surface effects in real nanoparticles. The dependence of the MW field on the energy landscape might be used to address directly a given nanoparticle in a polydisperse assembly.

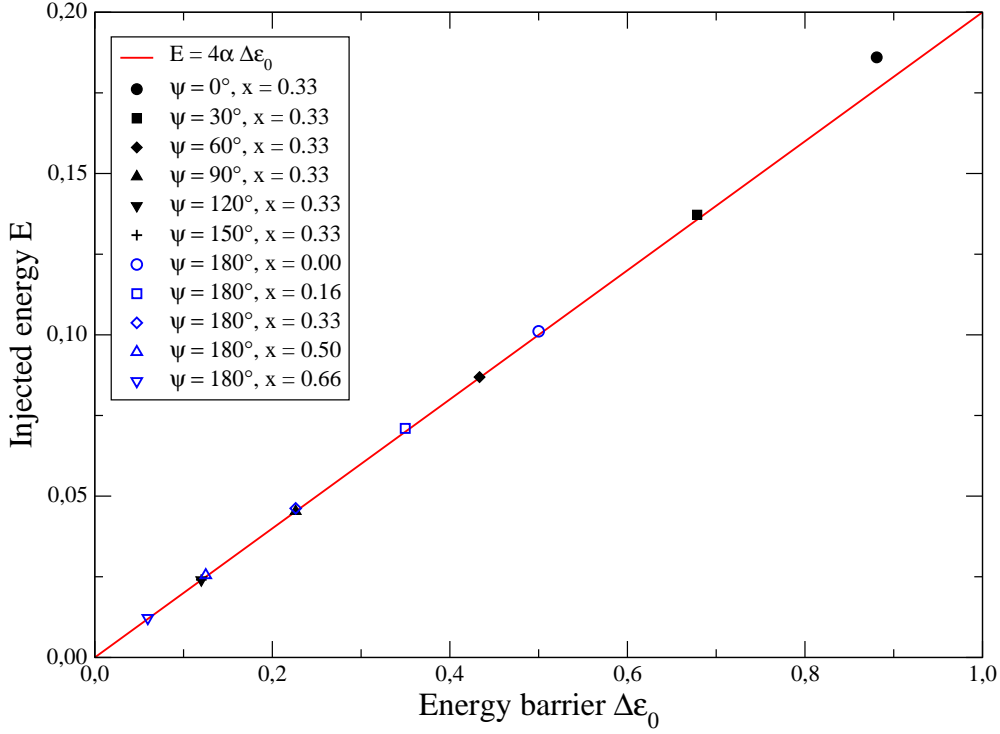


Figure 5: Total injected energy E with respect to the static energy barrier $\Delta\mathcal{E}_0$ for varying magnitude and orientation of the static field \mathbf{h} . ψ is the angle between the z axis (anisotropy axis) and the static field and $x = h/k$.

ACKNOWLEDGMENTS

We are grateful to our collaborators E. Bonet, C. Thirion (Institut Néel, Grenoble, France) and V. Dupuis (LPMCN, Lyon, France) for instructive discussions on the microwave-assisted switching of isolated nanoclusters. This work has been funded by the collaborative program PNANO ANR-08-P147-36 of the French Ministry.

¹ T. Thomson, L. Abelman, and H. Groenland, in *Magnetic Nanostructures in Modern Technology*, edited by B. Azzarboni, G. Asti, L. Pareti, and M. Ghidini (Springer Netherlands, ADDRESS, 2008), pp. 237–306.

² C. Thirion, W. Wernsdorfer, and D. Mailly, *Nat. Mat.* **2**, 524 (2003).

³ Z. Z. Sun and X. R. Wang, *Phys. Rev. B* **74**, 132401 (2006).

⁴ Z. Z. Sun and X. R. Wang, *Phys. Rev. B* **73**, 092416 (2006).

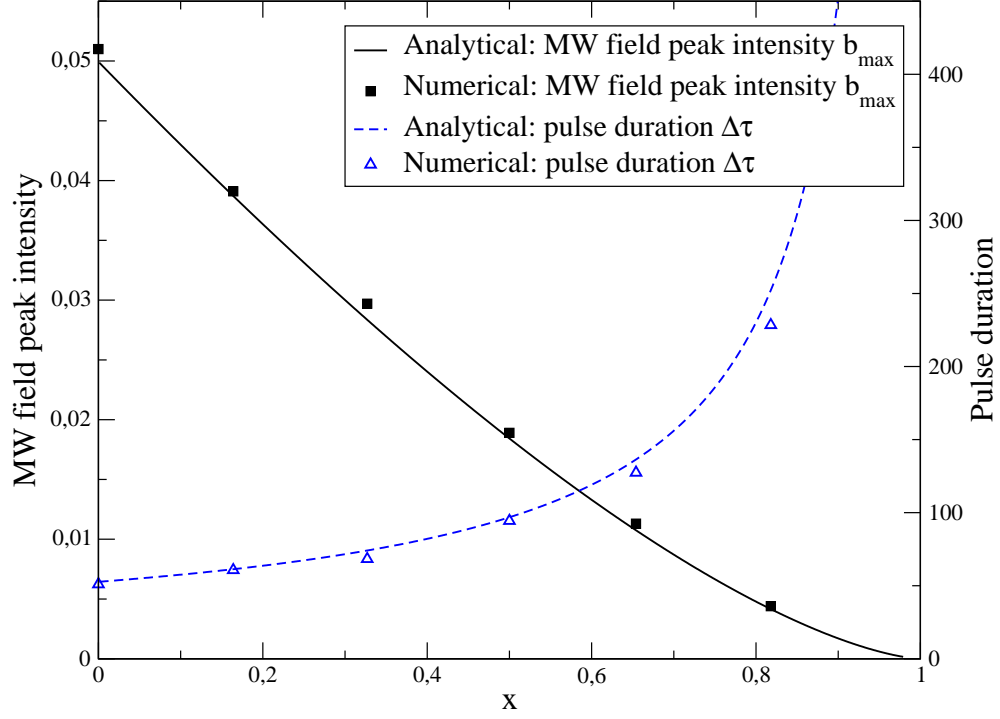


Figure 6: Case of a longitudinal static field: maximal peak intensity and peak duration of the optimal MW field for varying magnitude of the static field $x = h/k$.

⁵ G. Woltersdorf and C. H. Back, Phys. Rev. Lett. **99**, 227207 (2007).

⁶ B. Meerson and L. Friedland, Phys. Rev. A **41**, 5233 (1990).

⁷ S. Okamoto, N. Kikuchi, and O. Kitakami, Applied Physics Letters **93**, 142501 (2008).

⁸ L. Cai, D. A. Garanin, and E. M. Chudnovsky, Phys. Rev. B **87**, 024418 (2013).

⁹ N. Barros, M. Rassam, H. Jirari, and H. Kachkachi, Phys. Rev. B **83**, 144418 (2011).

¹⁰ D. A. Garanin and H. Kachkachi, Phys. Rev. Lett. **90**, 065504 (2003).

¹¹ H. Kachkachi and E. Bonet, Phys. Rev. B **73**, 224402 (2006).

¹² R. Yanes *et al.*, Phys. Rev. B **76**, 064416 (2007).

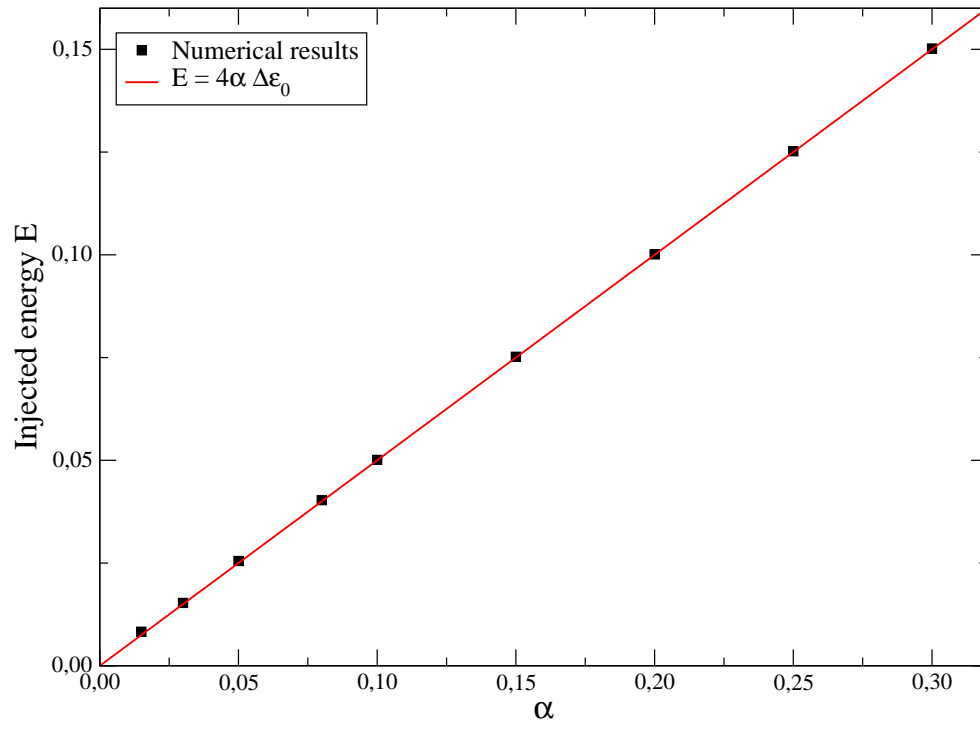


Figure 7: Total injected energy E with respect to the damping parameter α .

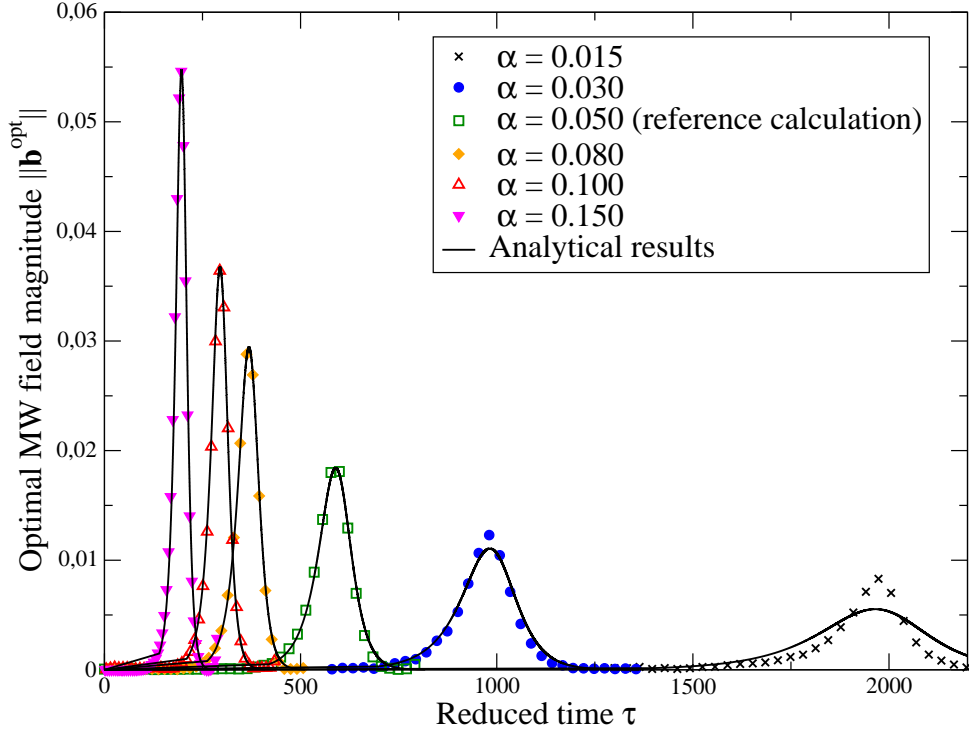


Figure 8: Optimal MW field pulse for several values of the damping parameter α . For $\alpha = 0.015$, the final time has been increased ($\tau_f = 1600$) without changing the sampling time.